THE JOURNAL OF COMPARATIVE NEUROLOGY 505:586–601 (2007)

Distinct Populations of Presympathetic-Premotor Neurons Express Orexin or Melanin-Concentrating Hormone in the Rat Lateral Hypothalamus

ILAN A. KERMAN,* RENÉ BERNARD, DEVIN ROSENTHAL, JAMES BEALS, HUDA AKIL, AND STANLEY J. WATSON
Molecular and Behavioral Neuroscience Institute, University of Michigan, Ann Arbor, Michigan 48109

ABSTRACT

Orexin and melanin-concentrating hormone (MCH) have been implicated in mediating a variety of different behaviors. These include sleep and wakefulness, locomotion, ingestive behaviors, and fight-or-flight response, as well as anxiety- and panic-like behaviors in rodents. Despite such diversity, all these processes require coordinated recruitment of the autonomic and somatomotor efferents. We have previously mapped the locations of presympathetic-premotor neurons (PSPMNs) in the rat brain. These putative dual-function neurons send trans-synaptic projections to somatomotor and sympathetic targets and likely participate in somatomotor-sympathetic integration. A significant portion of these neurons is found within the dorsomedial (DMH) and lateral hypothalamus (LH), areas of the brain that contain MCH- and orexin- synthesizing neurons in the central nervous system. Thus, we hypothesized that hypothalamic PSPMNs utilize MCH or orexin as their neurotransmitter. To test this hypothesis, we identified PSPMNs by using recombinant strains of the pseudorabies virus (PRV) for trans-synaptic tract tracing. PRV-152, a strain that expresses enhanced green fluorescent protein, was injected into sympathectomized gastrocnemius muscle, whereas PRV-BaBlu, which expresses β-galactosidase, was injected into the adrenal gland in the same animals. By using immunofluorescent methods, we determined whether co-infected neurons express MCH or orexin. Our findings demonstrate that PSPMNs synthesizing either MCH or orexin are present within LH, where they form two separate populations. PSPMNs located around the fornix express orexin, whereas those located around the cerebral peduncle are more likely to express MCH. These two clusters of PSPMNs within LH likely play distinct functional roles in autonomic homeostasis and stress coping mechanisms. J. Comp. Neurol. 505:586–601, 2007.

Indexing terms: somatomotor-sympathetic integration; somatomotor control; central autonomic circuits; pseudorabies virus; peptides; transneuronal tracing

Orexins (orexin-A and orexin-B; also known as hypocretin 1 and hypocretin 2, respectively) were initially discovered as ligands for two orphan G-protein-coupled receptors (de Lecea et al., 1998; Sakurai et al., 1998). These peptides are derived from a common precursor molecule, prepro-orexin, which is cleaved to form orexin-A (33 amino acids long) and orexin-B (28 amino acids) (Sakurai et al., 1998; Willie et al., 2001). In their initial report Sakurai et al. (1998) described the structure of these peptides and demonstrated that they stimulate short-term food intake. Subsequent investigations have confirmed that these peptides stimulate arousal and feeding behavior in rats and mice (Edwards et al., 1999; Haynes et al., 2000, 2002) and have also implicated them in the regulation of emotion, energy homeostasis, reward, and drug addiction (Yamanaka et al., 2003; Akiyama et al., 2004; Boutrel et al., 2005; Harris et al., 2005; Narita et al., 2006; Sakurai,

Grant sponsor: the Pritzker Neuropsychiatric Disorders Research Consortium; Grant sponsor: National Institutes of Health; Grant number: P01 MH042251 (to S.J.W.); Grant sponsor: the University of Michigan Comprehensive Depression Center Innovation Fund Grant Program (to I.A.K. and R.B); Grant sponsor: The Mental Health Research Association (NARSAD) Young Investigator Award (to I.A.K.).

*Correspondence to: Ilan A. Kerman, Molecular and Behavioral Neuroscience Institute, 205 Zina Pitcher Place, University of Michigan, Ann Arbor, MI 48109. E-mail: kerman@umich.edu

Received 25 April 2007; Revised 2 July 2007; Accepted 23 August 2007
DOI 10.1002/cne.21511
Published online in Wiley InterScience (www.interscience.wiley.com).

2007). It has also been demonstrated that the orexins participate in regulating locomotor activity as part of motivated behaviors, such as foraging for food following fasting (Yamanaka et al., 2003) and that they are part of an integrated cardiovascular and locomotor response to acute stress (Zhang et al., 2006). In addition, intracerebroventricular administration of orexin-A leads to increases in mean arterial pressure and heart rate in awake behaving rats (Samson et al., 2007).

Orexin-synthesizing neurons in the central nervous system are found exclusively within the lateral (LH) and dorsomedial (DMH) hypothalamic nuclei (Sakurai et al., 1998; Swanson et al., 2005). Within these regions, orexin-synthesizing neurons are intermingled with those neurons that synthesize melanin-concentrating hormone (MCH). Although these two populations of hypothalamic neurons are located within the same areas, they are neurochemically distinct, as MCH-positive cells do not synthesize orexins and vice versa (Bayer et al., 2002; Swanson et al., 2005).

MCH is also located in the lateral hypothalamus and is a 19-amino-acid-long neuroactive peptide that is derived from the precursor prepro-MCH (Bittencourt et al., 1992). MCH was originally discovered in fish but has subsequently been identified in mammals, in whom it is thought to regulate energy balance (Pissios et al., 2006). In addition to energy balance, MCH neurotransmission has also been implicated in regulating locomotor activity (Marsh et al., 2002; Segal-Lieberman et al., 2003), and inactivation of the MCH receptor 1 leads to increased wheel running (Zhou et al., 2005). MCH neurotransmission is also thought to play a role in mediating anxiety- and depression-like behaviors in rodents (Borowsky et al., 2002). Furthermore, intracerebroventricular infusions of MCH increase rapid eye movement sleep (Verret et al., 2003) and produce bradycardic and hypotensive responses in rats (Messina and Overton, 2007), suggesting that MCH neurotransmission also participates in regulation of the autonomic nervous system and the sleep/wake cycle.

Taken together, these data suggest that orexins and MCH participate in coordinating activities of somatomotor and autonomic systems and that they do so within the context of motivated behaviors. We have previously used a virally mediated trans-synaptic tract-tracing approach to map the locations of neurons that send polysynaptic projections to skeletal muscle and to the adrenal gland (Kerman et al., 2003, 2006a,b). We have proposed that these neurons (referred to here as *presympathetic-premotor neurons* [PSPMNs]) have dual functions in regulating activities of the sympathetic and somatomotor systems. Although PSPMNs are widely distributed throughout the brain, major clusters of these neurons are found within areas thought to mediate motivated behaviors such as responses to stress (Kerman et al., 2003, 2006a,b). Such areas include LH and DMH, both regions that have been implicated in mediating stress responses as well as regulating food intake (Kerman et al., 2006a). These areas also contain all the orexin-synthesizing neurons and the majority of MCH-synthesizing neurons in the central nervous system (Bittencourt et al., 1992; Sakurai et al., 1998).

Thus, given the proposed role of PSPMNs in regulating physiological aspects of motivated behaviors and the known role of orexins and MCH in coordinating somatomotor and autonomic functions, we hypothesized that a subset of hypothalamic PSPMNs synthesize orexins or MCH. To test this hypothesis we identified PSPMNs by using our previously developed retrograde trans-synaptic tract-tracing paradigm and then used triple-label immunofluorescence to determine whether these cells synthesize orexins or MCH.

MATERIALS AND METHODS

All the procedures regarding animal use in this study conformed to the Guide for the Care and Use of Laboratory Animals of the NIH and were approved by the University of Michigan's University Committee on Use and Care of Animals.

Antibody specificity and distribution of MCH- and orexin-synthesizing neurons

In our initial experiments we sought to compare the distribution of MCH- and orexin-synthesizing neurons in the rat brain. Adult male Sprague-Dawley rats (n = 2; Charles River, Wilmington, MA) were used in these studies. Animals were deeply anesthetized with 1 ml i.p. of 50 mg/ml pentobarbital sodium solution and transcardially perfused with 100–150 ml of physiological saline followed by 400–500 ml of a 4% paraformaldehyde solution containing 1.4% l-lysine and 0.2% sodium meta-periodate (PLP) (McLean and Nakane, 1974). Brains were then extracted, postfixed in PLP overnight, and immersed in 20% sucrose until they sank to the bottom of the container. Tissue was then sectioned coronally on a freezing microtome at a thickness of 40 μm and collected into six adjacent bins. Tissue was then stored at −20°C in cryoprotectant (30% sucrose, 30% ethylene glycol, 1% polyvinyl-pyrrolidine [PVP-40]) until immunohistochemical processing was conducted.

To study the distribution of MCH-positive neurons, we used rabbit anti-MCH serum (Phoenix Pharmaceuticals, Burlingame, CA, cat. #: H-070-47, lot #: 00606). This antibody was raised against full-length peptide (sequence: Asp-Phe-Asp-Met-Leu-Arg-Cys-Met-Leu-Gly-Arg-Val-Tyr-Arg-Pro-Cys-Trp-Gln-Val) and has been shown to have 100% cross-reactivity against MCH and 0% cross-reactivity against orexins, agouti-related peptide, leptin, α-melanocyte-stimulating hormone, and neuropeptide Y (manufacturer's technical information).

To prevent nonspecific binding, tissue was first soaked in blocking solution that consisted of 0.3% Triton X-100 (TX-100), 1% normal goat serum (NGS), and 1% bovine serum albumin (BSA) in 0.1 M phosphate buffer (PB; pH 7.4). The antibody was then dissolved in the same blocking mix and reacted with tissue at 1:10,000 or 1:15,000 for 1 hour at room temperature followed by 48 hours at 4°C. The tissue was then reacted with biotinylated goat anti-rabbit IgG (Vector, Burlingame, CA) at 1:200 in blocking solution for 2 hours at room temperature. Following a brief rinse in 0.1 M PB, the tissue was then reacted with the VectaStain ABC System (Vector), with A and B reagents dissolved at 1:200 each in blocking solution. The reaction was then visualized with 0.04% diaminobenzedine (DAB) as chromogen and 2×10^{-5} % H_2O_2 in 0.1 M sodium acetate.

To verify the specificity of this antibody further, we performed a blocking study in which adjacent sections were incubated with the rabbit anti-MCH serum (as described above) and with rabbit anti-MCH serum preincu-

bated with 50 μM of the MCH peptide (Phoenix Pharmaceuticals, cat. #: 070-47, lot #: 424859).

To study the distribution of orexin-synthesizing neurons, we used an antibody raised against orexin-A. We used rabbit polyclonal antibody (Abcam, Cambridge, MA, cat. #: ab6214, lot #: 38610), which was raised against a synthetic peptide (sequence: Cys-Arg-Leu-Tyr-Glu-Leu-Leu-His-Gly-Ala-Gly-Asn-His-Ala-Ala-Gly-Ile-Leu-Thr-Leu), corresponding to amino acids 14–33 of cow orexin-A, and conjugated to Lys-Leu-His by a glutaraldehyde linker (manufacturer's technical information). This peptide has 100% amino acid identity with rat orexin-A, and it contains three regions of identity with orexin-B for a total of 13 identical amino acid residues between orexin-A and orexin-B (Sakurai et al., 1998). This antibody has been extensively tested to show that it cross-reacts to detect both orexin-A and orexin-B and that it only stains orexin-synthesizing neurons (Nambu et al., 1999). Tissue was incubated with this antibody diluted to 1:5,000 and then processed and visualized as described above.

Overview of tract-tracing studies

Male Sprague-Dawley rats (n = 11; Charles River) were used in tract-tracing studies. In these experiments we employed transgenic recombinants of an attenuated pseudorabies virus (PRV) strain, PRV-Bartha, for transneuronal tracing of multisynaptic pathways innervating adrenal gland and gastrocnemius muscle. PRV has preferential tropism for axonal terminals (Vahlne et al., 1978, 1980). It is transported in the retrograde direction from the terminals to the cell body where the viral genome is replicated in the nucleus (Enquist et al., 1998). Capsids are assembled and filled with viral DNA in the nucleus, acquire the mature envelope from a late Golgi compartment, and are transported to sites of afferent synaptic contact, where cell-to-cell retrograde transneuronal transmission of infection occurs (Card et al., 1993; Enquist et al., 1998). The two viral recombinants that we employed were PRV-152 and PRV-BaBlu. Both are derived from PRV-Bartha, which is an attenuated form of the parental strain, PRV-Becker. PRV-BaBlu contains the *lac Z* gene at the gG locus and produces β-galactosidase (β-gal) under the control of the viral gG promoter (Kim et al., 1999). PRV-152 carries the gene coding for enhanced green fluorescent protein (eGFP) at the gG locus, which is constitutively expressed under control of the cytomegalovirus immediate early promoter (Smith et al., 2000). Previous studies have demonstrated that PRV-152 and PRV-BaBlu are transported transsynaptically in a retrograde manner, similarly to PRV-Bartha and that the two recombinants are capable of simultaneously co-infecting the same neuronal population (Standish et al., 1995; Billig et al., 1999, 2000, 2001; Smith et al., 2000; Kerman et al., 2003, 2006a).

We previously reported a robust negative correlation between the animal's weight and efficiency of infection of gastrocnemius motoneurons, with the largest rate of motoneuron infection in rats of intermediate size that weigh approximately 200 g (Kerman et al., 2003). Thus, animals in the current study were selected to weigh between 163 and 254 g for an average of 197 ± 8 g (mean ± SEM). Animals were anesthetized with either an inhalable or an injectable anesthetic protocol. In the former case anesthesia was induced with 5% isoflurane vaporized in 1–1.5 L/min of O_2 and maintained with a 1.5–2.5% concentration. Alternatively, animals were injected i.p. with a mix of ketamine and xylazine (60 mg/kg ketamine and 7 mg/kg xylazine). Once a surgical plane of anesthesia was achieved such that there was no spontaneous movement and there were no withdrawal responses to tail and/or foot pinch, hindlimb sympathectomy was performed.

In addition to somatic motor efferents, the hindlimb is also innervated by sympathetic efferents that project to blood vessels, sweat glands, and other smooth muscle targets (Jänig and McLachlan, 1992). To prevent infection of sympathetic pathways following injection of PRV-152 into the gastrocnemius muscle, the hindlimb was surgically sympathectomized in all animals by using a previously described approach (Kerman et al., 2003). Briefly, the lumbar sympathetic nerve was dissected via a ventral laparotomy and was extirpated from the level of the renal artery caudal to the bifurcation of the abdominal aorta. Neural plexuses running along the descending aorta and inferior vena cava were also stripped off under microscopic observation by using fine forceps. The abdominal aorta and the inferior vena cava were then swabbed with 10–20% phenol dissolved in ethylene glycol. The abdominal musculature was closed with sutures, and the overlying skin was closed with surgical staples. This procedure is effective at removing the large majority of sympathetic efferents to the hindlimb, as evidenced by the lack of infection in the intermediolateral cell column in the same animals that exhibited robust infections of lumbar motoneurons (Kerman et al., 2003, 2006a,b).

Following sympathectomy and a 2–10-day recovery period, the animals were reanesthetized and injected with PRV-152 into either their right (n = 2) or left (n = 9) gastrocnemius muscle. Following a 24–32-hour recovery period, the same rats were reanesthetized and were injected with PRV-BaBlu into their left adrenal glands. Choice of anesthetic regime had no effect on viral infection or transport.

At the conclusion of the survival period following transport of viral tracers, animals were deeply anesthetized with 1 ml i.p. of 50 mg/ml pentobarbital sodium solution and transcardially perfused with 100–150 ml of physiological saline followed by 400–500 ml of a 4% paraformaldehyde solution containing 1.4% l-lysine and 0.2% sodium meta-periodate (PLP) (McLean and Nakane, 1974).

Double-virus injections

Viral recombinants used in the present studies were harvested from pig kidney cell cultures at a titer of 10^8 to 10^9 pfu/ml. Viral stocks were aliquoted in 50-μl volumes and stored at −80°C. At the times of injection viral aliquots were removed from the freezer and kept on ice until immediately before injections.

To determine the location of neurons coordinating muscle contraction and autonomic activity, rats received injections of PRV-152 into their gastrocnemius muscles and injections of PRV-BaBlu into their adrenal glands. In each animal the gastrocnemius muscle was injected with 30 μl of PRV-152, which was divided into multiple injections of 1.0 μl. The adrenal gland was dissected via a left flank incision and gently separated from surrounding viscera and fat; the adjacent connective tissue was then retracted to facilitate access to the gland. Two or three injections of PRV-BaBlu were then made into the gland through a glass pipette attached to a 10-μl Hamilton syringe; the total volume of virus injected was 2–4 μl. Following each

injection the gland was swabbed with a cotton-tip applicator to decrease nonspecific viral spread. We previously demonstrated that this injection protocol produces an efficient infection of target neurons and does not result in spread of virus to non-target tissues (Kerman et al., 2003).

Injected animals were assigned to one of three groups: short, intermediate, and long survival times. In the short survival group (n = 3) rats survived for 121–122 hours following injection with PRV-152 and for 96–97 hours following PRV-BaBlu injection. We chose this survival time point because this is the earliest time point at which appreciable numbers of double-infected neurons are detected in the rat hypothalamus (Kerman et al., 2006a). Because a single replication cycle of the virus is 10–12 hours (Demmin et al., 2001), we therefore decided to extend the survival times by 10–12 hours to determine the maximal number of double-infected neurons that express MCH and orexins. Accordingly, in the intermediate survival group (n = 4) the animals survived for 132 or 136 and 108 or 112 hours following injections with PRV-152 and PRV-BaBlu, respectively. In the late survival group (n = 4) the animals survived for 143–144 and 111–120 hours following injections with PRV-152 and PRV-BaBlu, respectively.

Tissue processing

Following transcardial perfusion with PLP (see above), the entire brain was extracted and postfixed in PLP overnight. Brains were then immersed in 20% sucrose until they sank to the bottom of the container; they were sectioned coronally on a freezing microtome at a thickness of 35 or 40 μm and collected into six bins. Tissue was stored at −20°C in cryoprotectant until immunohistochemical processing was conducted.

For immunofluorescent detection in the brain, tissue was initially rinsed with 0.1 M PB several times at room temperature. It was then incubated for 1 hour in the blocking solution (1% NGS, 1% BSA, and 0.3% TX-100 in 0.1 M PB). Sections were then reacted with a cocktail of primary antibodies—chicken anti-GFP IgY (Abcam, product # 13970) at 1:2,000, mouse anti-β-gal IgG (Sigma, St. Louis, MO, product # G4644) at 1:1,000, and either rabbit anti-MCH at 1:10,000 or rabbit anti-orexin at 1:500—diluted in the above blocking solution. In each animal adjacent tissue bins were processed for orexin, GFP, β-gal triple-labeling and for MCH, GFP, β-gal triple-labeling. The chicken anti-GFP antibody was raised against recombinant full-length protein. This antibody yields a single band on Western blot and detects GFP in transgenic mice expressing GFP in lamina II of the spinal cord (manufacturer's technical information). We have previously determined absence of staining with this antibody in uninfected rat tissue sections (Kerman et al., 2006b). Mouse anti-β-gal antibody was developed in mouse peritoneal cavities by using β-gal purified from *E. coli* as the immunogen. Using Western blot, this antibody was shown to be specific for β-gal in its native form (116 kDa), and it reacts only with β-gal from *E. coli* (manufacturer's technical information). The specificity of this antibody in immunofluorescent experiments has been previously documented (Kerman et al., 2003).

Following 48-hour incubation at 4°C in the primary antibody solution, the tissue was rinsed several times with 0.1 M PB and then reacted with a secondary antibody solution, which consisted of donkey anti-mouse IgG conjugated to CY3 (1:200; Jackson ImmunoResearch, West Grove, PA), goat anti-chicken IgG conjugated to Alexa Fluor 488 (1:200; Molecular Probes Invitrogen, Carlsbad, CA), and goat anti-rabbit IgG conjugated to Alexa Fluor 647 (1:200; Molecular Probes Invitrogen) dissolved in the blocking solution (1% NGS, 1% BSA, and 0.3% TX-100). Following processing, tissue sections were mounted on glass slides and coverslipped with Aqua Poly/Mount (Polysciences, Warrington, PA).

Tissue analysis

Images of antibody-labeled MCH and orexin-synthesizing neurons were taken at 10× magnification with a flat-field correction by using a Zeiss Axiophot upright light microscope (Carl Zeiss MicroImaging, Thornwood, NY), operated by a Ludl motorized stage that was connected to a Ludl MAC2000 XYZ controller module (Ludl Electronic Products, Hawthorne, NY). Images of individual fields of view were stitched together by using the virtual slice tool in Stereo Investigator software (MicroBrightField, Williston, VT) on a Dell PC.

Immunofluorescently labeled tissue was examined by using a Leica DMR photomicroscope (Wetzlar, Germany) and with an Olympus FluoView 1000 laser scanning confocal microscope (http://www.olympusfluoview.com/). Swanson's (2004) rat atlas was used as a reference for anatomical classification. When using Leica DMR microscope, the presence of each fluorophore was detected by using specific filter sets (Chroma Technology, Brattleboro, VT) with the following respective excitation and emission ranges: Alexa Fluor 488, 440–520 nm and 500–555 nm (green fluorescence); CY3, 535–560 nm and 545–625 nm (red fluorescence); and Alexa Fluor 647, 560–680 nm and 625–775 nm (far red fluorescence).

Adjacent black-and-white images of the LH were digitized under a 20× objective; images were then stitched together by using the Photomerge function in Adobe Photoshop CS (Adobe Systems, San Jose, CA). Each of these large stitched images corresponded to a different fluorescent filter set and was pseudocolored as follows: GFP-positive neurons, green; β-gal-containing cells, red; and MCH- or orexin-positive neurons, blue or cyan. These pseudocolored images were then overlaid, and colocalization of two or three fluorophores was determined by turning each layer on and off to determine location and color of each cell. Brightness and contrast of images were optimized for presentation purposes, and figures were prepared in Photoshop.

Statistical analyses

Potential differences in distribution of labeled neurons between perifornical and peripeduncular regions were evaluated with repeated measures ANOVA with region (perifornical vs. peripeduncular) and anatomical level as independent variables and percentage of cells that were either MCH-positive PSPMNs or orexin-positive PSPMNs as a dependent variable. Statistical analyses were carried out in StatView 5.0 (SAS Institute, Cary, NC), and significance was set as $P < 0.05$.

RESULTS

Specificity of the MCH antibody

To confirm the specificity of the MCH antibody, we performed a blocking study with the specific MCH peptide.

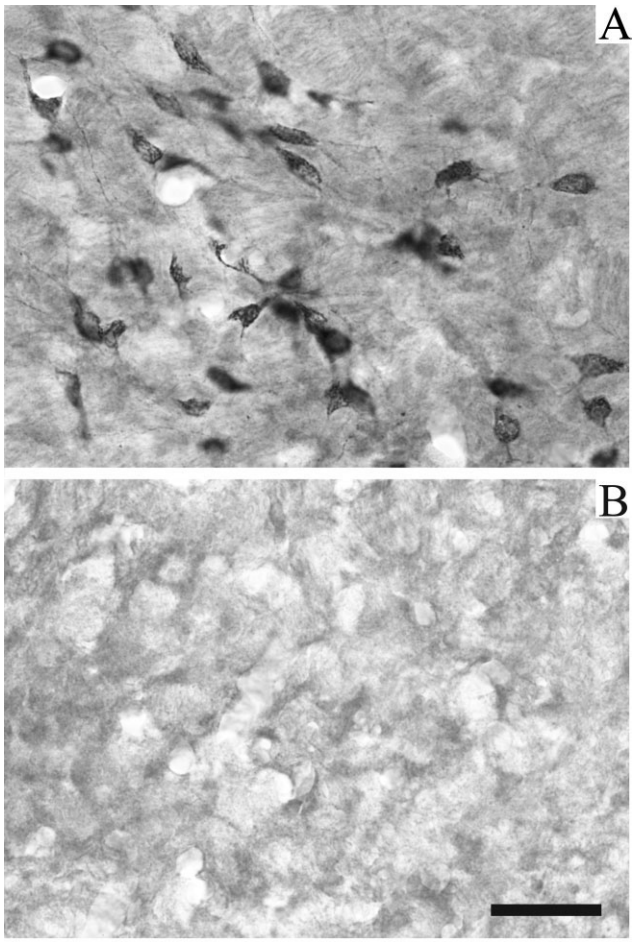

Fig. 1. Characterization of the MCH antiserum. Specificity was ascertained by performing a blocking study. Adjacent sections were incubated with the MCH antibody alone (**A**) or with MCH antibody preincubated with MCH peptide (**B**). Note robust labeling in A and absence of labeling in B, indicating specificity of the antibody binding. Scale bar = 50 μm in B (applies to A,B).

In this experiment, sections through the LH were reacted with the anti-MCH antibody with and without preincubation of MCH peptide. Under control conditions we detected robust labeling in LH around the cerebral peduncle (Fig. 1A). The observed MCH antibody labeling was completely abolished by preincubation with the MCH peptide (Fig. 1B), thus confirming the specificity of this antibody for MCH.

Distribution of MCH- and orexin-synthesizing neurons

Distribution of MCH- and orexin-synthesizing neurons was studied in sections from adjacent (1 in 6 series) bins that were visualized by using DAB as the chromogen. These studies demonstrated that although MCH-positive neurons were distributed throughout LH, they formed two clear groupings. The first cluster of MCH neurons was located around the fornix (perifornical region), whereas the second cluster of these cells was found around the cerebral peduncle (peripeduncular region). Figure 2A–C demonstrates this distribution pattern of MCH-positive neurons in LH. Note the clustering of neurons in the perifornical and peripeduncular regions, which is especially prominent at the caudal level that we examined (Fig. 2A).

Although orexin-positive neurons occupied a similar area within LH, it was apparent that the bulk of these neurons was located more medially than the MCH-positive cells. Figure 2D–F illustrates the distribution of orexin-positive cells; note that these neurons are preferentially distributed within the perifornical region compared with the peripeduncular region. Within the perifornical region, orexin-positive cells also appeared to be more prevalent than the MCH-positive cells (compare the labeling in Fig. 2F with that in Fig. 2C).

Expression of MCH within PSPMNs

In line with our previous observations (Kerman et al., 2006a), we detected considerable numbers of double-infected neurons within LH and DMH across all three survival groups. Within LH these neurons were equally distributed throughout the nucleus and were as likely to be located in the perifornical region as in the peripeduncular region.

We conducted triple-labeling experiments aimed at determining whether hypothalamic PSPMNs expressed MCH. In these experiments MCH-positive neurons were tagged with a far red fluorophore and were pseudocolored cyan. Cells that send polysynaptic projections to hindlimb muscle were tagged with a green fluorophore, and those that send polysynaptic projections to the adrenal gland were tagged with a red fluorophore. Thus, double-infected neurons appeared yellow, whereas triple-labeled neurons appeared as a mixture of all three colors.

Figure 3 illustrates examples of neurons infected with PRV-152 (green), or PRV-BaBlu (red), or both (yellow) and their relationship to the MCH-synthesizing neurons (cyan). We detected MCH within PSPMNs throughout LH; however, these triple-labeled cells appeared to be more numerous within the peripeduncular region (Fig. 3D2) than within the perifornical region (Fig. 3D1).

We then mapped the locations of MCH-positive PSPMNs, as well as the locations of neurons that were infected with only one PRV strain but also expressed MCH. These maps were created at three different rostrocaudal levels of the rat hypothalamus and across the three different survival periods used in the current study. Figure 4 illustrates the distributions of these cells at different survival times. Note that at the earliest survival time there are considerable numbers of PSPMNs in LH and DMH (Fig. 4A). Some of these neurons express MCH (black circles) and are intermingled with MCH-negative PSPMNs (yellow squares). Furthermore, these neurons are present around the fornix (in the perifornical region) and around the cerebral peduncle (in the peripeduncular region).

With increased survival time, the numbers of detected double-infected neurons increased and these cells were present throughout LH and DMH. However, with these longer survival times MCH-positive PSPMNs (black circles) segregated preferentially toward the peripeduncular region (Fig. 4B,C).

Expression of orexins within PSPMNs

We conducted triple-labeling experiments to determine whether hypothalamic PSPMNs are orexinergic. In these

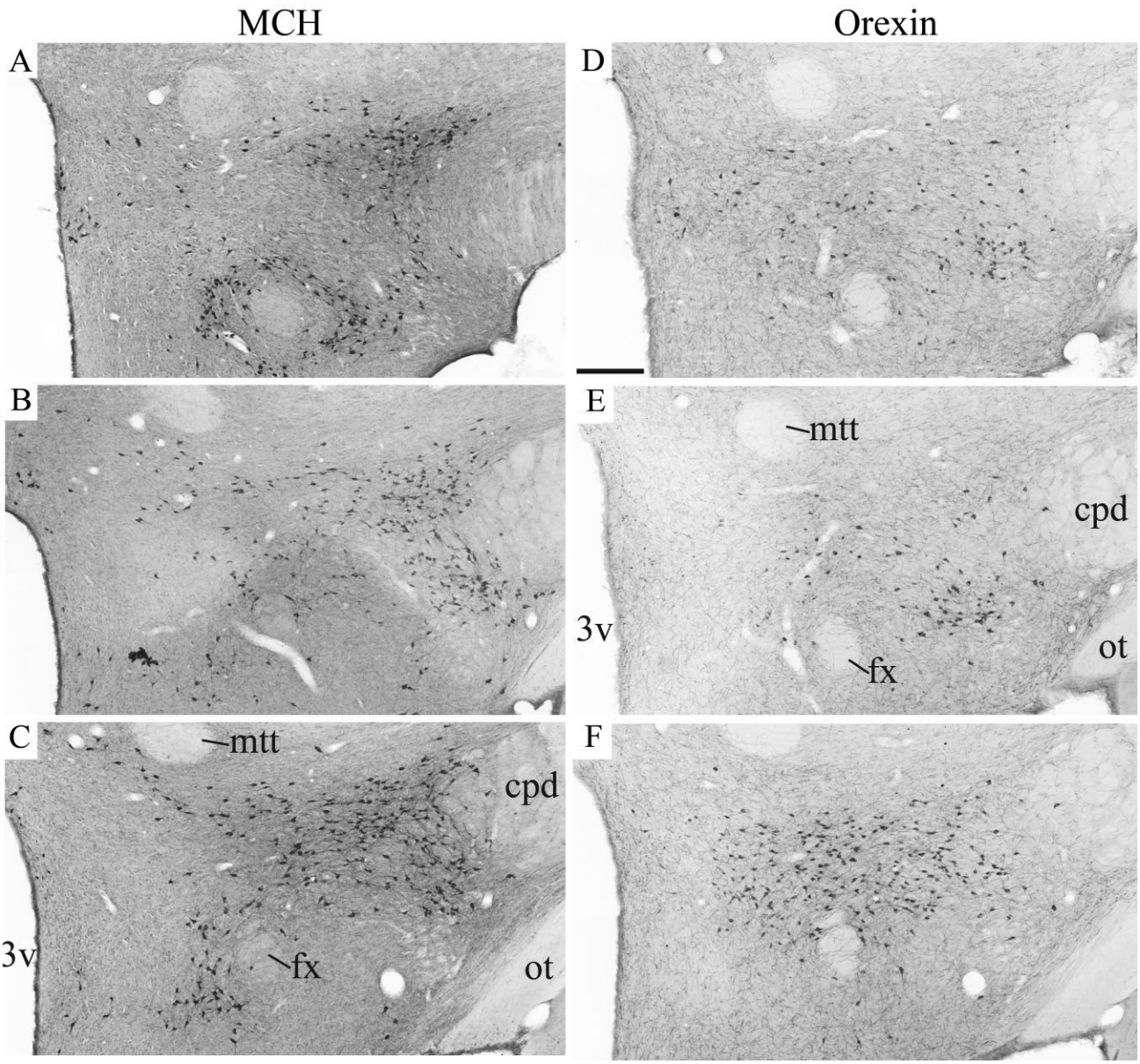

Fig. 2. Distribution of MCH- and orexin-positive neurons. Distribution of these neurons was examined at three rostrocaudal levels: approximately −3.80 mm (A,D; level 1), −3.25 mm (B,E; level 2), and −2.50 mm (C,F; level 3) from bregma. MCH-positive neurons are shown on the left (**A–C**), and orexin-positive neurons are shown on the right (**D–F**). Note the clustering of MCH-positive neurons around the fornix and at the medial edge of the cerebral peduncle, which is especially pronounced at the caudalmost level (A). Although orexinergic neurons are distributed throughout the lateral hypothalamus, they tend to cluster in the perifornical region. This is especially prominent at the rostralmost level (F). Abbreviations: 3v, third ventricle; cpd, cerebral peduncle; fx, fornix; mtt, mammillothalamic tract; ot, optic tract. Scale bar = 300 μm in D (applies to A–F).

experiments orexin-positive neurons were tagged with a far red fluorophore and pseudocolored cyan. Neurons that send polysynaptic projections to hindlimb muscle were tagged with a green fluorophore, whereas those sending polysynaptic projections to the adrenal gland were tagged with a red fluorophore. Figure 5 illustrates data from these experiments; note that in these examples the numbers of orexin-positive PSPMNs are greater within the perifornical area (Fig. 5D1) compared with the peripeduncular area (Fig. 5D2).

As with the MCH-positive neurons, we mapped the locations of orexin-positive PSPMNs in relation to the orexin-negative double-infected neurons as well as to orexin-positive single-infected neurons (Fig. 6). This mapping revealed that orexin-positive PSPMNs were detected even at the earliest survival time point and that the numbers of double-infected cells increased with longer survival times. Furthermore, as the numbers of PRV-infected neurons increased with increasing survival, orexin-positive

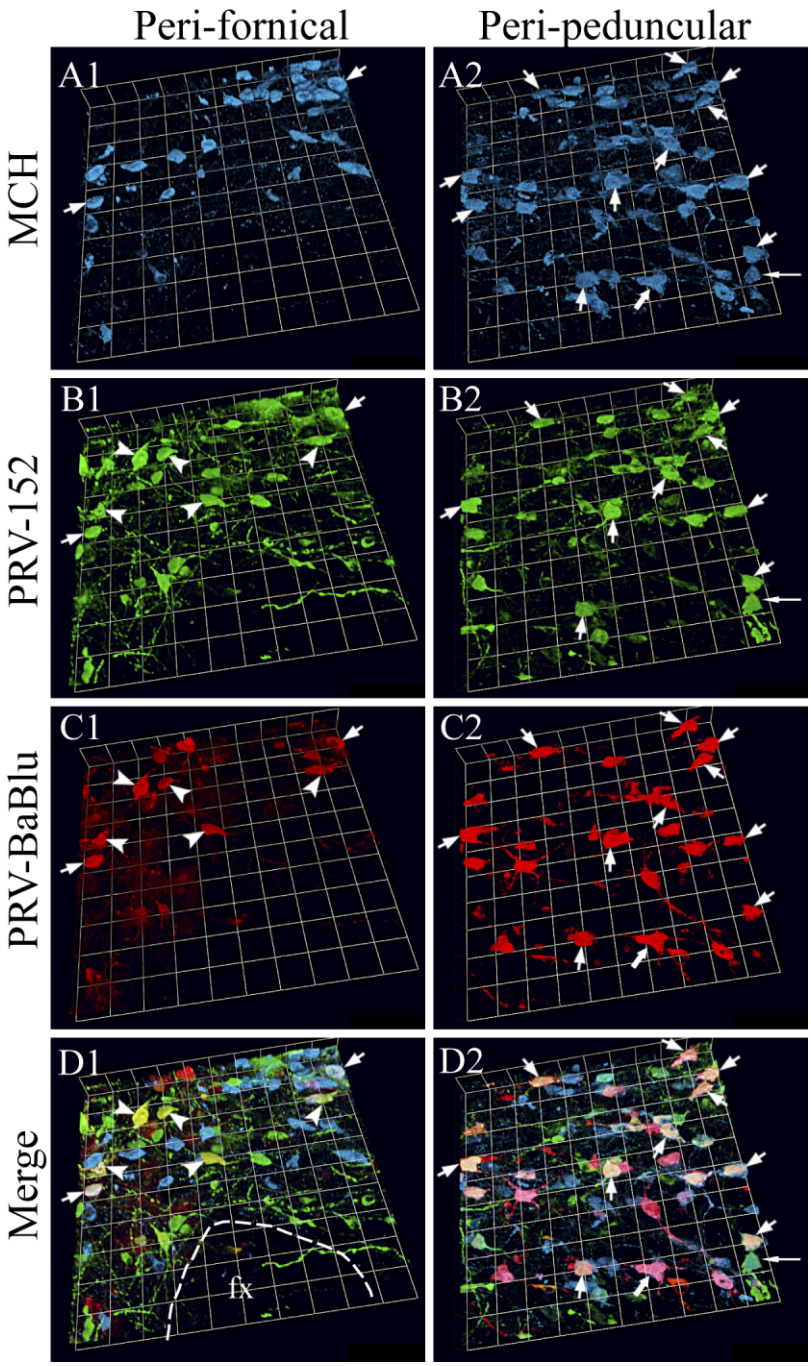

Fig. 3. Co-localization of viral reporter genes with melanin-concentrating hormone (MCH) in neurons of the lateral hypothalamus. Triple-labeled sections were imaged with a laser-scanning confocal microscope taking 40–60 optical sectioins per field of view. For each image the z-stack was compressed, and images were rendered for three-dimensional representation. **A1,A2:** MCH-positive neurons were tagged with Alexa Fluor 647 and pseudocolored with cyan. **B1,B2,C1,C2:** Hypothalamic neurons that send polysynaptic projections to hindlimb muscle were infected with pseudorabies virus (PRV)-152, tagged with Alexa Fluor 488, and pseudocolored with green (B1,B2); neurons with polysynaptic projections to the adrenal gland were infected with PRV-BaBlu, tagged with CY3, and pseudocolored with red (C1,C2). **D1,D2:** Merged images of A1–C2. **A1–D1:** Images from the perifornical region (note the edge of the fornix outlined with a dashed line). **A2–D2:** Images from the peripeduncular region. Triple-labeled neurons (MCH-positive PSPMNs) are shown with arrows. An MCH-positive neuron that was infected only with PRV-BaBlu is shown with thick arrows in A2–D2, and an MCH-positive neuron that was infected only with PRV-152 is shown with long narrow arrows in A2–D2. Double-infected neurons that are MCH-negative are shown with arrowheads. Note greater numbers of triple-labeled neurons in the peripeduncular region (2) compared with the perifornical region (1). Abbreviation as in Figure 2. Each box of the grid is 32 μm.

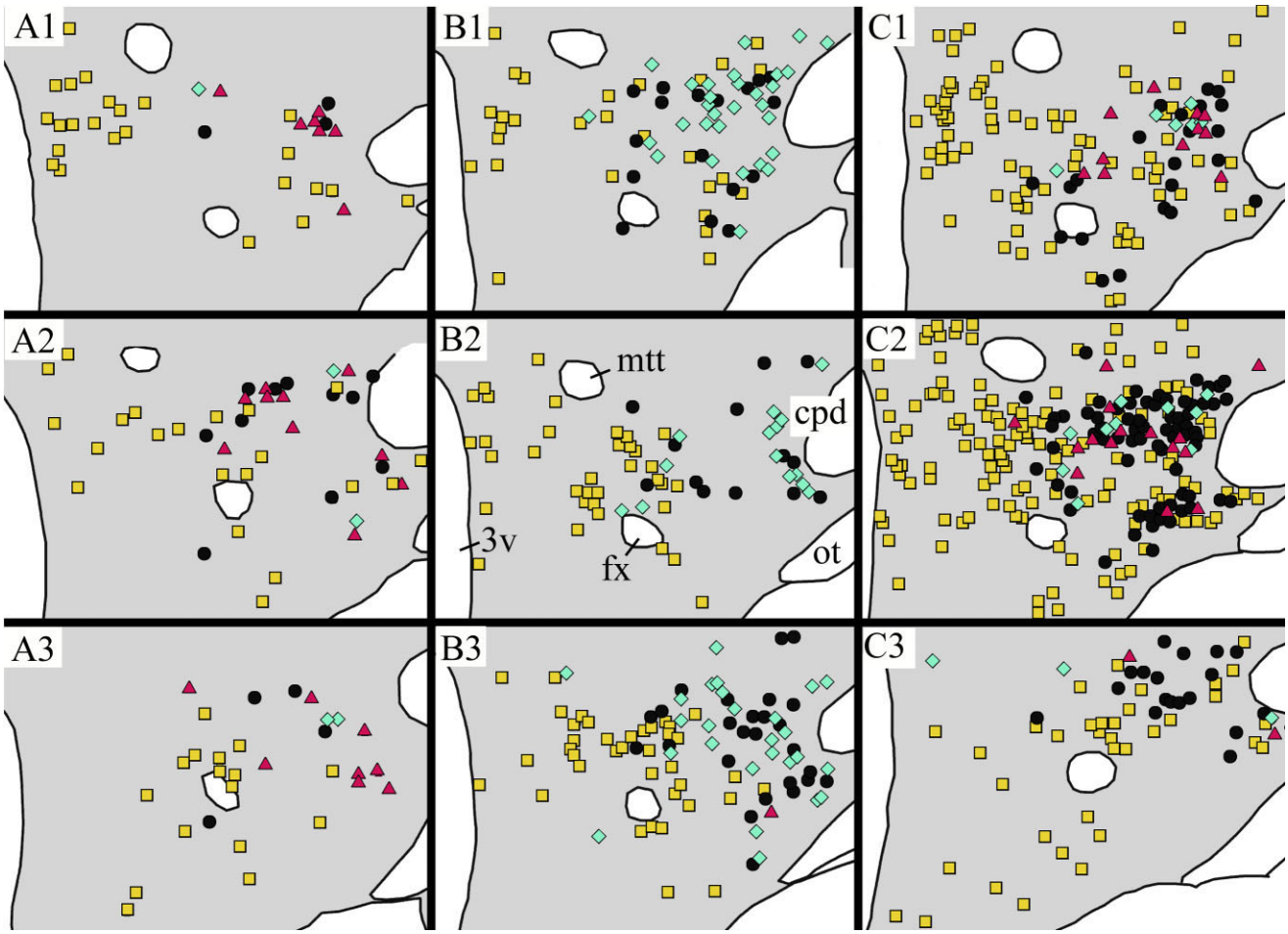

Fig. 4. Distribution of MCH- and PRV-containing neurons in the hypothalamus. Anatomical landmarks were traced from original sections, and locations of virus-infected cells were plotted onto these maps. Only one hemisection is presented from each level, but the pattern of labeling was symmetrical. Each symbol represents one neuron on the actual section. Yellow squares represent neurons co-infected with PRV-152 (polysynaptic projections to hindlimb muscle) and PRV-BaBlu (polysynaptic projections to adrenal gland). Black circles represent neurons co-infected with PRV-152 and PRV-BaBlu that also express MCH. Red triangles represent MCH-containing neurons that are infected only with PRV-BaBlu, and aqua diamonds indicate MCH-containing neurons infected only with PRV-152. Labeling was examined at three rostrocaudal levels (similar to the ones represented in Figure 2: 1, caudal; 2, intermediate; 3, rostral. Panels on the left (**A1–A3**) are from an animal in the short survival group, those in the middle (**B1–B3**) are from an animal in the intermediate survival group, and those on the right (**C1–C3**) are from an animal in the long survival group. Note that although double-infected neurons are distributed throughout the lateral and dorsomedial hypothalamus, PSPMNs that express MCH are preferentially distributed in the peripeduncular region (along the medial edge of cerebral peduncle). This is especially prominent at longer survival time points (for example, C2). Abbreviations as in Figure 2.

PSPMNs preferentially clustered within the perifornical region of LH (Fig. 6B,C).

Comparison of the distribution of MCH- and orexin-positive PSPMNs

To compare the distribution of MCH- and orexin-positive PSPMNs directly, double-infected neurons that were positive for each of these peptides were mapped onto corresponding atlas plates from Swanson's (2004) rat brain atlas. Figure 7 illustrates data from this mapping study; at each survival time point MCH- and orexin-positive PSPMNs were projected onto the same atlas plate (plate #30 in Swanson's (2004) rat brain atlas. These data demonstrate a clear segregation of MCH- (red dots) and orexin- (blue dots) synthesizing PSPMNs into lateral and medial clusters, respectively. This clustering is apparent at intermediate (Fig. 7B) and long (Fig. 7C) survival time points.

To determine whether this segregation into medial and lateral groups of orexin- and MCH-positive PSPMNs is true throughout the rostrocaudal extent of LH, we performed the same mapping procedure at three different rostrocaudal levels for data collected from two of the long-surviving animals. Figure 8 illustrates results from this study; these data also indicate segregation of MCH- and orexin-positive PSPMNs into lateral and medial groups within LH.

Quantification

To determine regional differences in the distribution of PRV-infected neurons, we quantified the numbers of: 1)

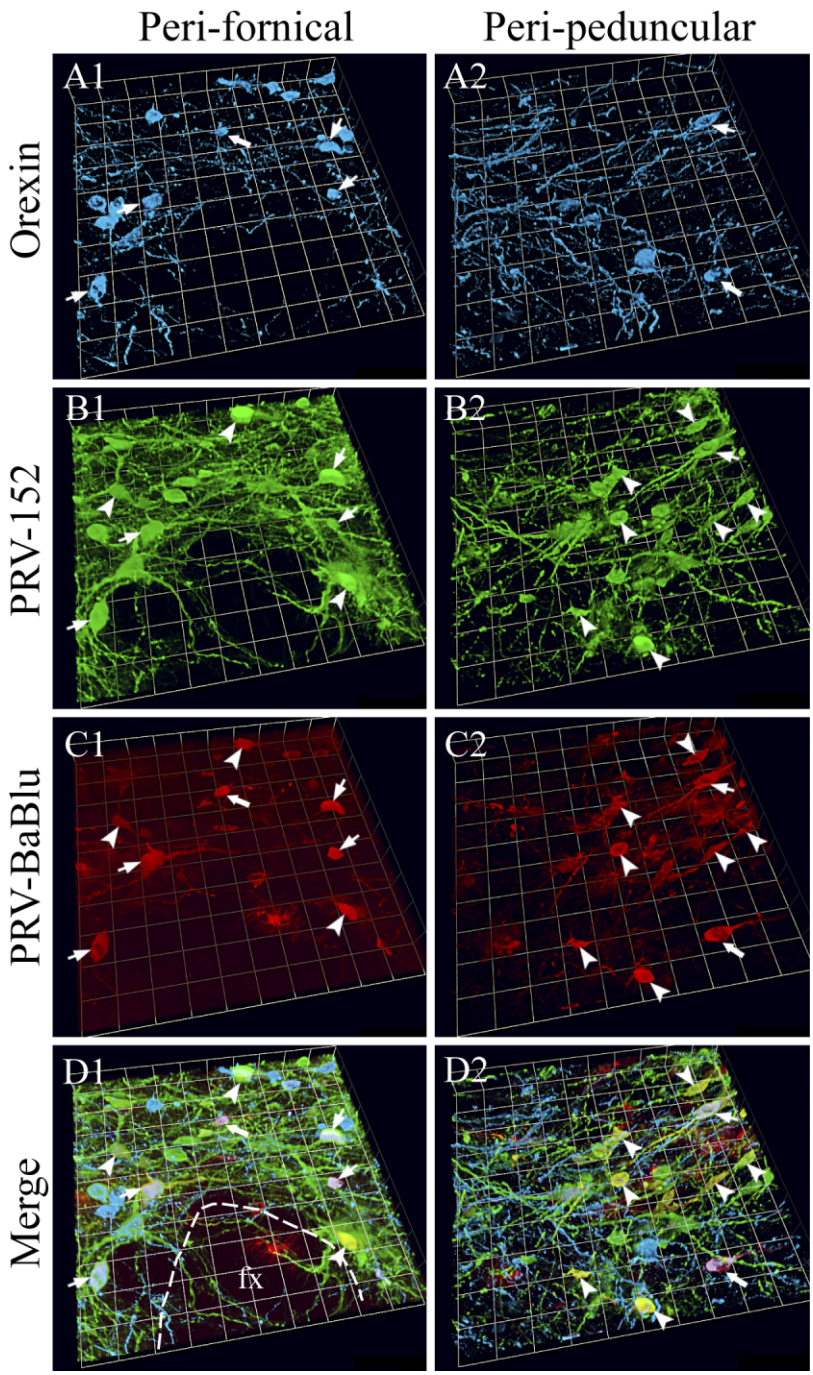

Fig. 5. Co-localization of viral reporter genes with orexin in neurons of the lateral hypothalamus. Triple-labeled sections were imaged with a laser-scanning confocal microscope taking 40–60 optical sections per field of view. For each image the z-stack was compressed, and images were rendered for three-dimensional representation. **A1,A2:** Orexin-positive neurons were tagged with Alexa Fluor 647 and pseudocolored with cyan. **B1,B2,C1,C2:** Hypothalamic neurons that send polysynaptic projections to hindlimb muscle were infected with pseudorabies virus (PRV)-152, tagged with Alexa Fluor 488, and pseudocolored with green (B1,B2); neurons with polysynaptic projections to the adrenal gland were infected with PRV-BaBlu, tagged with CY3, and pseudocolored with red (C1,C2). **D1,D2:** Merged images of A1–C2. **A1–D1:** Images from the perifornical region (note the edge of the fornix outlined with a dashed line). **A2–D2:** Images from the peripeduncular region. Triple-labeled neurons (orexin-positive PSPMNs) are shown with arrows. Double-infected neurons that are orexin-negative are shown with arrowheads. Thick arrows in A1–D1 and A2–D2 show orexin-positive neurons that were infected only with PRV-BaBlu. Note greater numbers of triple-labeled neurons in the perifornical region (1) compared with the peripeduncular region (2). Images were taken from the same animal as shown in Figure 4. Abbreviation as in Figure 2. Each box of the grid is 32 μm.

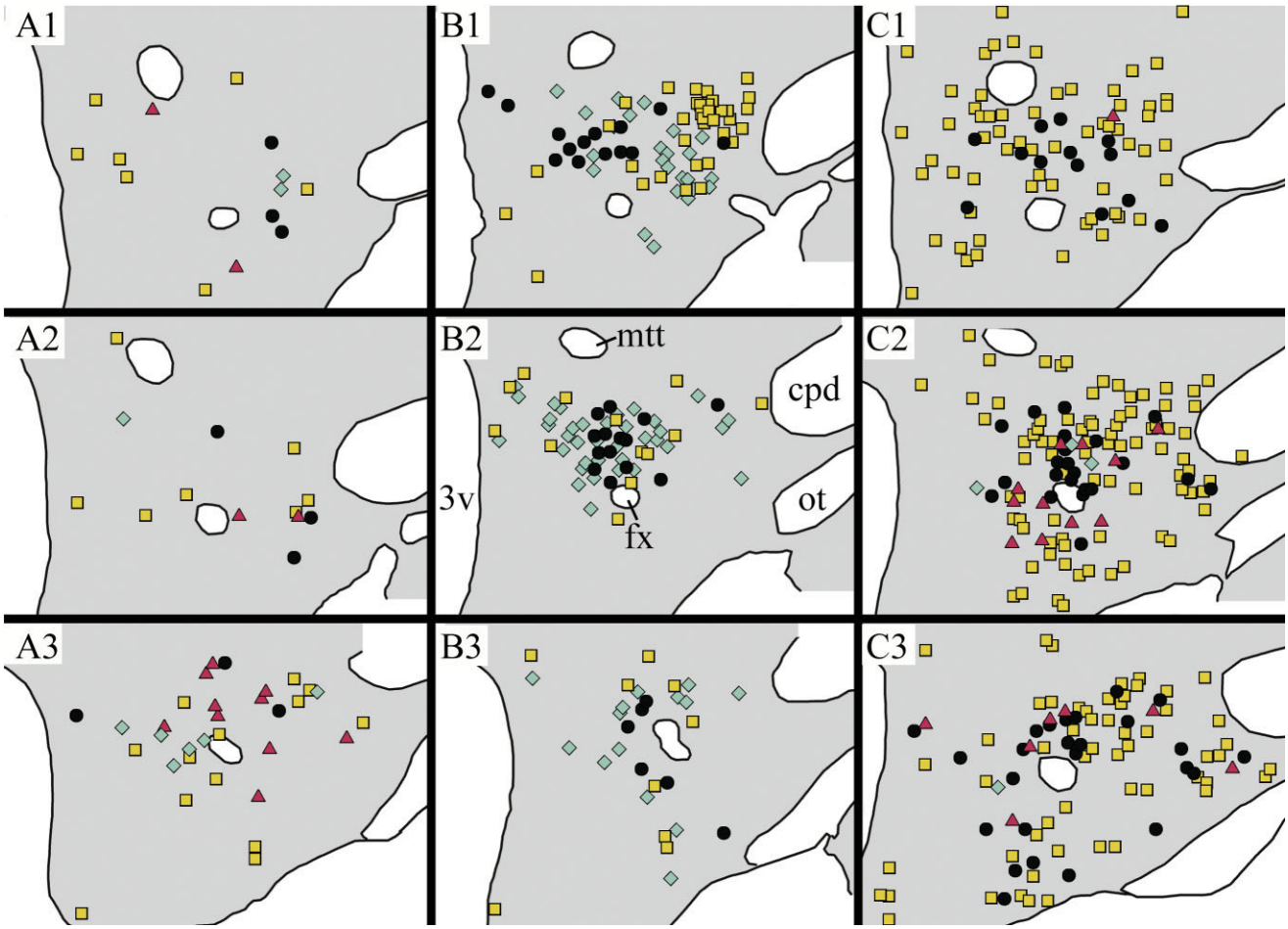

Fig. 6. Distribution of orexin- and PRV-containing neurons in the hypothalamus. Anatomical landmarks were traced from original sections, and locations of virus-infected cells were plotted onto these maps. Only one hemisection is presented from each level, but the pattern of labeling was symmetrical. Each symbol represents one neuron on the actual section. Yellow squares represent neurons co-infected with PRV-152 (polysynaptic projections to hindlimb muscle) and PRV-BaBlu (polysynaptic projections to adrenal gland). Black circles represent neurons co-infected with PRV-152 and PRV-BaBlu that also express orexin. Red triangles indicate orexin-containing neurons that are infected only with PRV-BaBlu, and aqua diamonds indicate orexin-containing neurons infected only with PRV-152. Labeling was examined at three rostrocaudal levels similar to the ones represented in Figure 2: 1, caudal; 2, intermediate; 3, rostral. Panels on the left (**A1–A3**) are from an animal in the short survival group, those in the middle (**B1–B3**) are from an animal in the intermediate survival group, and those on the right (**C1–C3**) are from an animal in the long survival group. Note that although double-infected neurons are distributed throughout the lateral and dorsomedial hypothalamus, orexin-positive PSPMNs are preferentially distributed in the perifornical region (e.g., in C2). Abbreviations as in Figure 2.

double-infected neurons that were MCH- or orexin-negative; 2) double-infected neurons that were MCH- or orexin-positive; and 3) neurons that were infected with only one of the PRV strains and were either MCH- or orexin-positive. This procedure was carried out in tissue obtained from three rats from the intermediate survival time point. This survival time was chosen because it is the first time point at which appreciable numbers of double-infected neurons are detected that probably send direct projections to the spinal cord. Quantification was performed on sections from three different anatomical levels, as illustrated in Figure 2.

Digitized tissue sections were marked up with different symbols representing these combinations of markers (see Figs. 4 and 6 for examples). These maps were then projected onto digital plates from the Swanson's (2004) rat atlas, and symbols were counted within the different hypothalamic nuclei (Tables 1, 2). Based on Swanson's atlas, the following LH subnuclei were grouped together to represent the peripeduncular region: dorsal region; ventral region, lateral zone; ventral region, medial zone; magnocellular nucleus; and parvicellular region. In addition, the preparasubthalamic nucleus was also included in the peripeduncular region. For the perifornical region, the posterior hypothalamus was included as well as the following LH subnuclei: juxtadorsomedial; suprafornical; juxtaventromedial region, dorsal zone; and juxtaventromedial region, ventral zone.

To evaluate potential differences in the distribution of MCH-positive PSPMNs between perifornical and peripeduncular regions, cell counts for each anatomical level in each animal were expressed as percentage of total neu-

rons that were detected (these included MCH-positive PSPMNs, MCH-negative PSPMNs, and neurons that were infected with only one of the PRV strains and expressed MCH). Figure 9A illustrates these data. Potential differences in the distribution of MCH-positive PSPMNs between perifornical and peripeduncular subdivisions were evaluated with repeated measures ANOVA with region (peripeduncular vs. perifornical) and anatomical level as independent variables and percentage of cells as a dependent variable. The ANOVA revealed significant differences in distribution of cells by region ($F = 23.390$, df 1, 8, $P < 0.01$), and no effects of level ($P > 0.1$) or level by region interaction ($P > 0.1$).

To evaluate potential differences in the distribution of orexin-positive PSPMNs between perifornical and peripeduncular regions, cell counts for each anatomical level in each animal were expressed as percentage of total neurons that were detected (these included orexin-positive PSPMNs, orexin-negative PSPMNs, and neurons that were infected with only one of the PRV strains and expressed orexin). Figure 9B illustrates these data. Potential differences in the distribution of orexin-positive PSPMNs between perifornical and peripeduncular subdivisions were evaluated with repeated measures ANOVA with region (peripeduncular vs. perifornical) and anatomical level as independent variables and percentage of cells as a dependent variable. The ANOVA revealed significant differences in distribution of cells by region ($F = 16.414$, df 1, 8, $P < 0.05$), and no effects of level ($P > 0.1$) or level by region interaction ($P > 0.1$).

DISCUSSION

In the current paper we focused our attention on hypothalamic PSPMNs. Neurons with putative dual (sympathetic and somatomotor) functions were identified by injecting distinct PRV recombinants into hindlimb muscle and the adrenal gland. Based on our previous reports on the anatomical distribution of the hypothalamic PSPMNs, we hypothesized that a subset of these neurons would be MCH- or orexin-positive. To test this hypothesis, we carried out triple-labeling experiments in which we combined immunofluorescent detection of viral reporter genes with that of orexins and MCH. Our results demonstrate that dual-infected neurons synthesize both orexins (Figs. 5, 6) and MCH (Figs. 3, 4). Previous studies have demonstrated that orexin- and MCH-positive neurons constitute separate but intermixed populations (Broberger et al., 1998; Elias et al., 1998; Swanson et al., 2005); thus MCH- and orexin-positive PSPMNs comprise separate neuronal pop-

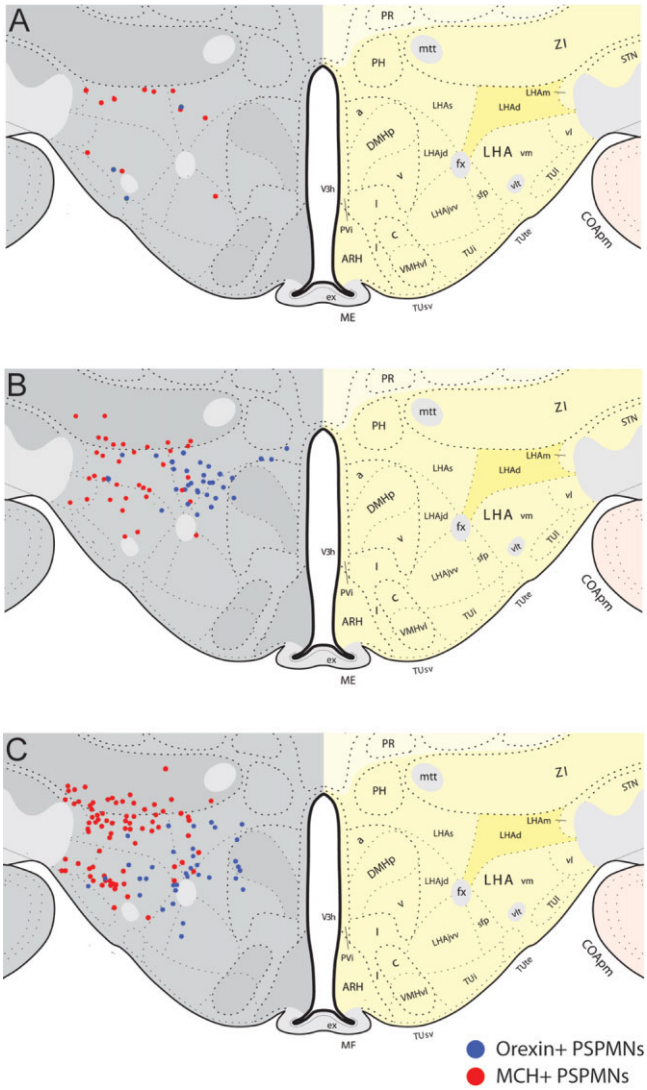

Fig. 7. Spatial segregation of melanin-concentrating hormone (MCH)- (red) and orexin- (blue) positive presympathetic-premotor neurons (PSPMNs). Each dot represents one neuron. Dual-infected neurons that were also MCH- or orexin-positive from adjacent sections were projected onto the same section taken from Swanson's rat brain atlas (plate #30, Swanson, 2000). **A:** Data taken from one animal in the short survival group. **B:** Data from two animals in the intermediate survival group. **C:** Data from two animals in the long survival group. Note that although there is some intermixing between the two populations, the majority of the two types of neurons are spatially segregated. Melanin-concentrating hormone (MCH)-positive presympathetic-premotor neurons (PSPMNs) are distributed more laterally and closer to the medial edge of the cerebral peduncle, whereas orexin-positive PSPMNs are distributed more medially around the fornix and in the dorsomedial hypothalamus. Abbreviations: ARH, arcuate hypothalamic nucleus; COApm, cortical amygdalar nucleus, posterior part, medial zone; DMHa, dorsomedial hypothalamic nucleus, anterior part; DMHp, dorsomedial hypothalamic nucleus, posterior part; DMHv, dorsomedial hypothalamic nucleus, ventral part; fx, fornix; I, internuclear part, hypothalamic periventricular region; LHA, lateral hypothalamic area; LHAd, lateral hypothalamic area, dorsal region; LHAjd, lateral hypothalamic area, juxtadorsomedial region; LHAjvv, lateral hypothalamic area, juxtaventromedial region, ventral zone; LHAm, lateral hypothalamic area, magnocellular nucleus; LHAs, lateral hypothalamic area, suprafornical region; LHAsfp, lateral hypothalamic area, subfornical region, posterior zone; LHAvl, lateral hypothalamic area, ventral region, lateral zone; LHAvm, lateral hypothalamic area, ventral region, medial zone; MEex, median eminence, external lamina; mtt, mammillothalamic tract; PH, posterior hypothalamic nucleus; PR, perireuniens nucleus; PVi, periventricular hypothalamic nucleus, intermediate part; STN, subthalamic nucleus; TUi, tuberal nucleus, intermediate part; TUl, tuberal nucleus, lateral part; TUsv, tuberal nucleus, subventromedial part; TUte, tuberal nucleus, terete subnucleus; V3h, third ventricle, hypothalamic part; vlt, ventrolateral hypothalamic tract; VMHc, ventromedial hypothalamic nucleus, central part; VMHvl, ventromedial hypothalamic nucleus, ventrolateral part; ZI, zona incerta.

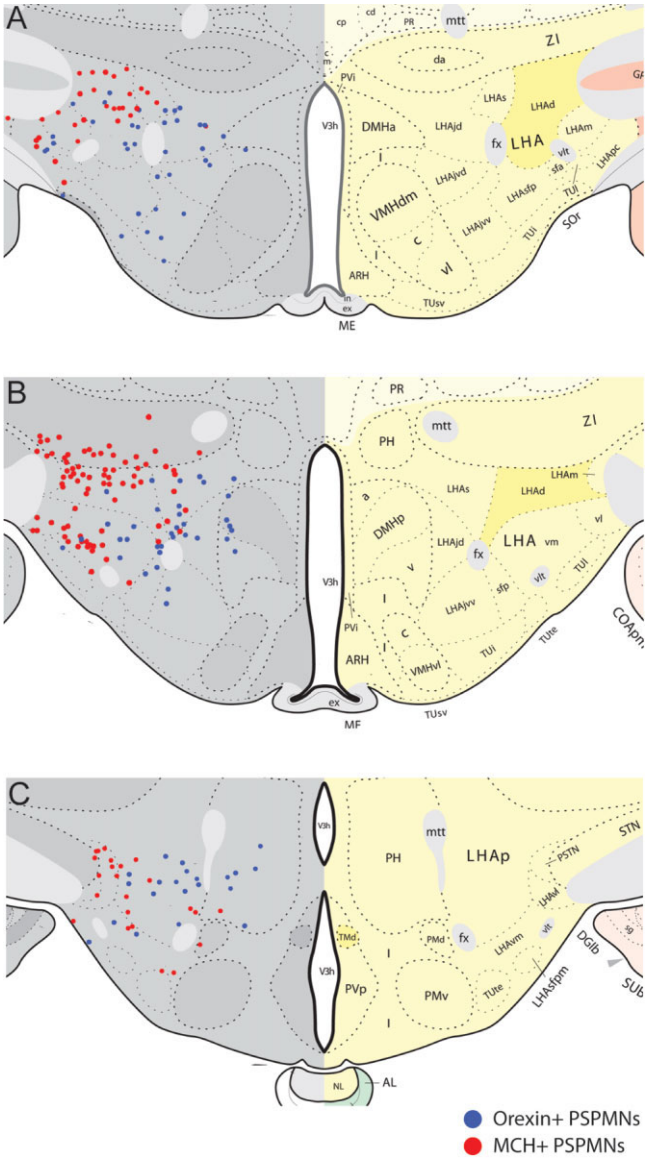

Fig. 8. Spatial segregation of MCH- (red) and orexin- (blue) positive PSPMNs. The layout of the figure is similar to that of Figure 8, except multiple sections from Swanson's (2004) rat brain atlas are represented. **A–C:** Data are shown rostral (A) to caudal (C), with A corresponding to plate 28 of the atlas, B corresponding to plate 30, and C corresponding to plate 32. Data were taken from two animals at the long survival time. Note the spatial segregation of the two populations of PSPMNs, with MCH-positive cells lying more laterally and orexin-positive cells distributed more medially. Abbreviations: AL, pituitary gland, anterior lobe; DGlb, dentate gyrus, lateral blade; DGlb-sg, dentate gyrus, lateral blade-granule cell layer; LHAsfpm, lateral hypothalamic area, subfornical region, permammillary zone; NL, pituitary gland, neural lobe; PMd, dorsal premammillary nucleus; PMv, ventral premammillary nucleus; PSTN, parasubthalamic nucleus; PVp, periventricular hypothalamic nucleus, posterior part; SUB, subiculum; TMd, tuberomammillary nucleus, dorsal part. For other abbreviations, see Figure 7 legend.

ulations. Our data are consistent with this interpretation and extend it further by demonstrating that orexin- and MCH-positive PSPMNs are spatially segregated. Accordingly, such orexin-positive neurons are distributed mainly within the perifornical region of LH, whereas MCH-positive PSPMNs are found primarily within its peripeduncular subdivision.

TABLE 1. Number of Neurons Infected With PRV and Their Co-Localization With MCH at the Intermediate Survival Time Point Within the Peripeduncular and Perifornical Regions of the Lateral Hypothalamus[1]

Anatomical level	Label	Peripeduncular	Perifornical
1	MCH+PRV-152+PRV-BaBlu	11.7 ± 7.7	2.0 ± 2.0
	PRV-152+PRV-BaBlu	5.7 ± 3.2	5.0 ± 5.0
	MCH+PRV-BaBlu	1.7 ± 0.9	0
	MCH+PRV-152	7.3 ± 3.2	1.0 ± 1.0
2	MCH+PRV-152+PRV-BaBlu	15.0 ± 6.5	0.7 ± 0.3
	PRV-152+PRV-BaBlu	10.7 ± 2.3	17.3 ± 4.2
	MCH+PRV-BaBlu	3.3 ± 1.7	0
	MCH+PRV-152	7.7 ± 3.4	1.3 ± 0.7
3	MCH+PRV-152+PRV-BaBlu	12.3 ± 3.2	3.3 ± 1.2
	PRV-152+PRV-BaBlu	10.7 ± 0.9	13.7 ± 5.9
	MCH+PRV-BaBlu	2.7 ± 1.2	1.0 ± 0.6
	MCH+PRV-152	8.3 ± 4.9	1.7 ± 1.2

[1]Data are totals from three animals sacrificed at the intermediate survival time point. Anatomical levels 1, 2, and 3 refer to anatomical levels illustrated in Figure 2. Data are presented as mean ± SEM. See text for additional details. Abbreviations: MCH, melanin-concentrating hormone; PRV, pseudorabies virus.

TABLE 2. Number of Neurons Infected with PRV and Their Co-Localization With Orexin at the Intermediate Survival Time Point Within the Peripeduncular and Perifornical Regions of the Lateral Hypothalamus[1]

Anatomical level	Label	Peripeduncular	Perifornical
1	Orexin+PRV-152+PRV-BaBlu	2.7 ± 1.8	6.7 ± 2.7
	PRV-152+PRV-BaBlu	18 ± 7.6	10.7 ± 6.2
	Orexin+PRV-BaBlu	0.7 ± 0.7	1.0 ± 0.6
	Orexin+PRV-152	7.0 ± 4.2	4.0 ± 2.0
2	Orexin+PRV-152+PRV-BaBlu	4.3 ± 3.0	10.0 ± 2.0
	PRV-152+PRV-BaBlu	14.0 ± 10.0	19.0 ± 4.0
	Orexin+PRV-BaBlu	0.3 ± 0.3	4.7 ± 1.3
	Orexin+PRV-152	5.7 ± 2.3	2.3 ± 0.3
3	Orexin+PRV-152+PRV-BaBlu	1.7 ± 1.2	7.0 ± 3.1
	PRV-152+PRV-BaBlu	6.0 ± 3.1	6.7 ± 1.2
	Orexin+PRV-BaBlu	0.7 ± 0.3	1.3 ± 0.7
	Orexin+PRV-152	1.7 ± 0.7	5.7 ± 3.7

[1]Data are totals from three animals sacrificed at the intermediate survival time point. Anatomical levels 1, 2, and 3 refer to anatomical levels illustrated in Figure 2. Data are presented as mean ± SEM. See text for additional details. Abbreviation: PRV, pseudorabies virus.

Antibody specificity

For data interpretation it is important to consider first the specificity of the antibodies that were used in the current study. In regard to the antibodies used to detect viral reporter genes, we have previously confirmed their specificities by demonstrating absence of staining in non-infected rat brain tissue (Kerman et al., 2003, 2006a). Furthermore, the orexin antiserum employed in this current study has been extensively characterized by Nambu and co-workers (1999). As part of their study these authors demonstrated that preincubation of the serum with orexins, but not with neuropeptide Y or angiotensin, abolishes the signal (Nambu et al., 1999). Furthermore, they demonstrated staining with this antibody in cells transfected with prepro-orexin cDNA but not in the mock transfected cells (Nambu et al., 1999). Although we did not carry out such controls in our study, the pattern of distribution of orexinergic neurons that we observed in our material (Fig. 2D–F) was consistent with a previous description using both immunocytochemistry and in situ hybridization (Elias et al., 1998; Sakurai et al., 1998; Nambu et al., 1999; Swanson et al., 2005); thus we can be

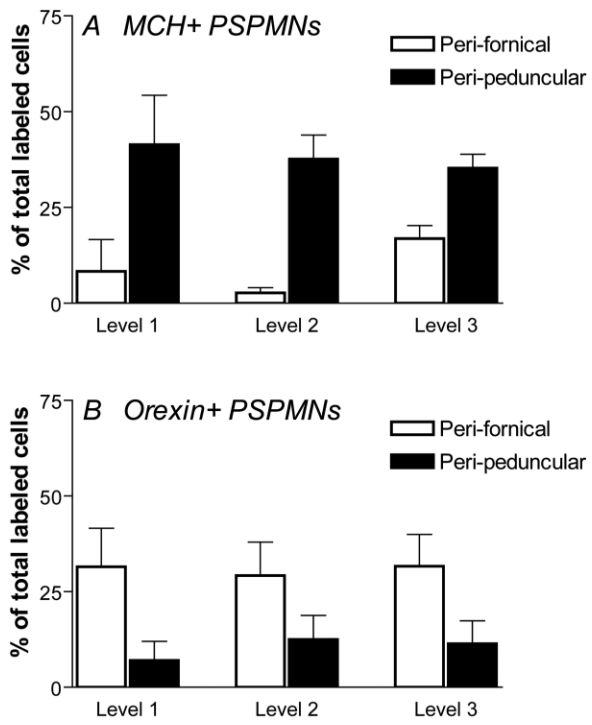

Fig. 9. Distribution of melanin-concentrating hormone (MCH)- (**A**) and orexin- (**B**) positive presympathetic-premotor neurons (PSPMNs) within perifornical and peripeduncular subregions. For each animal the numbers of triple-labeled neurons within the two subdivisions were expressed as percentages of the total number of neurons that were detected. These values were averaged and are presented as mean ± SEM. Levels 1, 2, and 3 refer to anatomical levels illustrated in Figure 2. Differences in the distribution of triple-labeled neurons between perifornical and peripeduncular regions were statistically significant for MCH and orexin: A (MCH-positive PSPMNs), $P < 0.01$, repeated measures ANOVA; B (orexin-positive PSPMNs), $P < 0.05$, repeated measures ANOVA. See text for additional details.

confident of the specificity of the orexin antiserum used in the present study.

The pattern of labeling that we observed with the MCH antibody used in the current study (Fig. 2A–C) was likewise similar to the pattern of distribution of this peptide that was previously described (Bittencourt et al., 1992; Elias et al., 1998; Swanson et al., 2005). We further verified the specificity of this antibody by performing a blocking study (Fig. 1) in which the antiserum was preincubated with the MCH peptide. Data from this experiment demonstrated the specificity of this antibody as the staining was completely abolished by the preincubation. Thus, we are also confident of the specificity of the MCH antiserum used in this study.

Connectional considerations

It is likely that at least some of the double-infected neurons that we identified in the present study send direct projections to the spinal cord. The presence of such neurons at the earliest survival time in our study is consistent with this notion. Furthermore, the presence of spinally projecting neurons in LH has also been demonstrated by using retrograde tract tracers (Hosoya, 1980; Haring and Davis, 1983; Kohler et al., 1984; Shiosaka et al., 1985; Porter and Brody, 1986). Therefore, it seems feasible that such hypothalamospinal neurons collateralize to innervate simultaneously adrenal sympathetic preganglionic neurons and lumbar motoneurons. This hypothesis is supported by anatomical investigations that demonstrated the existence of heavy density of orexinergic fibers in the intermediolateral column of the spinal cord and moderate density of these fibers in the ventral horn (van den Pol, 1999). The presence of MCH-immunoreactive fibers in the intermediolateral cell column and the lumbar ventral horn of the spinal cord has also been demonstrated (Bittencourt and Elias, 1998). Nonetheless, definitive demonstration of such collateralized projections directly from LH to the spinal cord requires further investigation.

In addition to the direct projections to the spinal cord, LH also contains neurons with projections to the lower brainstem. Among them are neurons that innervate the ventromedial medulla (Hosoya, 1985), which is the most likely site of this relay because this area contains the greatest numbers of the caudally located PSPMNs (Kerman et al., 2003, 2006b). Thus, it is likely that at least some of the double-infected neurons that we observed at longer survival times synapse on neurons in the ventromedial medulla, which in turn send descending projections to the spinal cord.

One of the major findings of the present study is the spatial separation of orexin- and MCH-positive PSPMNs. The orexinergic dual-infected neurons were more likely to be distributed medially within LH in the perifornical region, whereas MCH-positive PSPMNs were more likely to be found closer to the medial edge of the cerebral peduncle (see Figs. 7 and 8). This finding is supported by traditional tract-tracing approaches using retrogradely transported fluorescent dyes to study ascending and descending projections from LH (Bittencourt and Elias, 1998). Bittencourt and Elias (1998) showed that descending MCH-positive neurons were distributed laterally within LH along the medial edge of the cerebral peduncle, whereas the ascending neurons were distributed more medially within the perifornical region (see Fig. 6 of their paper). Cvetkovic and colleagues (2004) have also demonstrated that MCH neurons express neurokinin-3 receptor and cocaine- and amphetamine-regulated transcript (CART). However, a distinct cluster of MCH neurons just medial to the cerebral peduncle does not express these markers (Cvetkovic et al., 2004). Based on their previous observations that neurokinin-3 receptor-negative MCH neurons send descending projections to the spinal cord, whereas neurokinin-3 receptor-positive neurons send ascending projections (Brischoux et al., 2002), these authors proposed parcellation of MCH neurons into two categories. According to this scheme, class A neurons are neurokinin-3 receptor- and CART-negative and have descending projections, whereas class B neurons are neurokinin-3 receptor- and CART-positive and have ascending projections (Cvetkovic et al., 2004). The finding that spinally projecting class A MCH neurons are located just medial to the cerebral peduncle strongly supports our current observation of clustering of MCH-positive PSPMNs in the peripeduncular LH.

Previous studies have also demonstrated that LH neurons sending polysynaptic projections to a variety of autonomically innervated targets synthesize orexins. For example, Geerling and colleagues (2003) demonstrated the presence of orexin double-labeled neurons within LH fol-

lowing PRV injections into stellate and celiac sympathetic ganglia, as well as following its injection into the adrenal gland and kidney. Closer examination of their data suggests that such double-labeled neurons tend to cluster more around the fornix than other areas in LH (see Figs. 1 and 2 in Geerling et al., 2003), which is consistent with our findings. Furthermore, a study by Krout and coworkers (2003) suggests that orexinergic perifornical neurons send collateralized polysynaptic projections to the motor cortex and to the central autonomic network.

Functional considerations

Previous studies (reviewed above) along with the data presented in the current paper suggest the existence of two distinct cell groups within LH—one located more laterally at the medial edge of the cerebral peduncle and one located more medially around the fornix. Although both of these cell groups contain neurons that send descending polysynaptic projections that collateralize to innervate hindlimb muscle and adrenal gland, the perifornical group is made up predominantly of orexinergic neurons, whereas the peripeduncular group is made up primarily of MCH-positive neurons.

Although we cannot directly evaluate the functional role of this separation from the present study, previous anatomical, physiological, and behavioral studies of LH offer some clues on the possible functional roles of these two cell groups. We have previously mapped the locations of PSPMNs throughout the central nervous system (Kerman et al., 2003, 2006a). Their pattern of distribution suggests that one of their possible functions is to coordinate activities of the somatomotor and sympathetic systems in response to stress. For example, a major cluster of such neurons is found within the paraventricular nucleus of the hypothalamus, which is the main neuroendocrine integrator of the stress response (Swanson and Kuypers, 1980; Herman and Cullinan, 1997; Reyes et al., 2003), as well as within the periaqueductal gray, which mediates motor and autonomic components of the "fight-or-flight" response to stress (Bandler et al., 1991; Keay and Bandler, 2004).

In animals, stress responses can generally be classified into either "active coping" or "passive coping" (Bandler et al., 2000). Active coping responses are usually elicited by escapable stressors such as the presence of a rival or a predator, whereas inescapable or uncontrollable stressors, such as deep muscular pain, elicit passive coping responses (Bandler et al., 2000). Active coping is characterized by increased somatomotor activity that is part of escape or fighting behavior, as well as a hypertensive response (Bandler et al., 2000). On the other hand, passive coping is characterized by general quiescence and hypotension (Bandler et al., 2000). Our data, taken together with previous physiological and behavioral studies, suggest that the perifornical orexinergic PSPMNs participate in the expression of the active coping response to stress, whereas the peripeduncular MCH-positive PSPMNs support the passive coping stress response.

The concept that orexin and MCH transmitter systems are involved in mediating stress responses is supported by findings that acute stressors induce Fos expression in orexinergic neurons (Winsky-Sommerer et al., 2004), whereas intracerebroventricular infusions of MCH increase anxiety-like behavior in mice on the elevated plus maze (Smith et al., 2006). Furthermore, chemical disinhibition of the perifornical area leads to increased blood pressure and heart rate, which are hallmarks of the fight-or-flight response; this effect is attenuated in orexin knockout mice (Kayaba et al., 2003). Likewise, awake behaving orexin knockout mice exhibit decreased cardiovascular and behavioral responses to acute social stressors (Kayaba et al., 2003). These data are in agreement with the concept that activity of the perifornical orexinergic PSPMNs participates in the expression of active coping stress responses.

In contrast to orexins, MCH neurotransmission likely plays a role in mediating quiescent or passive stress responses. Support for this notion comes from several lines of investigation. For example, melanin-concentrating hormone 1 receptor-deficient mice are hyperactive in their home-cages across a 24-hour period, suggesting that increased MCH transmission would lead to decreased levels of activity (Marsh et al., 2002). Furthermore, chronic intracerebroventricular administration of MCH leads to hypotension (Messina and Overton, 2007), a response that would be expected as part of a reaction to chronic inescapable stress. MCH neurons also express γ-aminobutyric acid (GABA)ergic characteristics, including synthetic enzymes for GABA synthesis and GABAergic receptors (Harthoorn et al., 2005; Hervieu, 2006). Finally, chemical stimulation with excitatory amino acid infusions within the peripeduncular portion of LH leads to hypotensive responses (Allen and Cechetto, 1992; Pajolla and de Aguiar Correa, 2004), whereas similar stimuli in the perifornical region lead to hypertensive responses (Allen and Cechetto, 1992). These stimulation sites correspond closely to the locations of MCH-positive and orexinergic PSPMNs identified in the present study.

CONCLUSIONS

In the current study we used a virally mediated transsynaptic tract-tracing approach to identify neurons with putative dual somatomotor-sympathetic function. These PSPMNs polysynaptically innervate adrenal gland and hindlimb muscle and likely participate in the expression of responses to stress. Our data indicate that these neurons form two distinct clusters within LH, those that synthesize orexins, which are located medially around the fornix, and those that express MCH, which are located laterally at the medial edge of cerebral peduncle. On the basis of previous studies, we hypothesize that these two groups of neurons are recruited differentially by different stressors. Orexinergic perifornical PSPMNs likely participate in active coping responses and may thus be recruited by escapable stressors, whereas MCH-positive peripeduncular PSPMNs likely participate in passive coping responses and may thus be recruited by inescapable stressors. Future investigations will be required to test this hypothesis.

ACKNOWLEDGMENTS

We are grateful to Mr. Cyrus Shabrang for his expert technical assistance. We also thank Dr. Sarah Clinton for a critical reading of an earlier version of this manuscript and for her help with statistical analysis.

LITERATURE CITED

Akiyama M, Yuasa T, Hayasaka N, Horikawa K, Sakurai T, Shibata S. 2004. Reduced food anticipatory activity in genetically orexin (hypocretin) neuron-ablated mice. Eur J Neurosci 20:3054–3062.

Allen GV, Cechetto DF. 1992. Functional and anatomical organization of cardiovascular pressor and depressor sites in the lateral hypothalamic area: I. Descending projections. J Comp Neurol 315:313–332.

Bandler R, Carrive P, Zhang SP. 1991. Integration of somatic and autonomic reactions within the midbrain periaqueductal grey: viscerotopic, somatotopic and functional organization. Prog Brain Res 87:269–305.

Bandler R, Price JL, Keay KA. 2000. Brain mediation of active and passive emotional coping Prog Brain Res 122:333–349.

Bayer L, Mairet-Coello G, Risold PY, Griffond B. 2002. Orexin/hypocretin neurons: chemical phenotype and possible interactions with melanin-concentrating hormone neurons. Regul Pept 104:33–39.

Billig I, Foris JM, Card JP, Yates BJ. 1999. Transneuronal tracing of neural pathways controlling an abdominal muscle, rectus, abdominis in the ferret. Brain Res 820:31–44.

Billig I, Foris JM, Enquist LW, Card JP, Yates BJ. 2000. Definition of neuronal circuitry controlling the activity of phrenic and abdominal motoneurons in the ferret using recombinant strains of pseudorabies virus. J Neurosci 20:7446–7454.

Billig I, Hartge K, Card JP, Yates BJ. 2001. Transneuronal tracing of neural pathways controlling abdominal musculature in the ferret. Brain Res 912:24–32.

Bittencourt JC, Elias CF. 1998. Melanin-concentrating hormone and neuropeptide EI projections from the lateral hypothalamic area and zona incerta to the medial septal nucleus and spinal cord: a study using multiple neuronal tracers. Brain Res 805:1–19.

Bittencourt JC, Presse F, Arias C, Peto C, Vaughan J, Nahon JL, Vale W, Sawchenko PE. 1992. The melanin-concentrating hormone system of the rat brain: an immuno- and hybridization histochemical characterization. J Comp Neurol 319:218–245.

Borowsky B, Durkin MM, Ogozalek K, Marzabadi MR, DeLeon J, Lagu B, Heurich R, Lichtblau H, Shaposhnik Z, Daniewska I, Blackburn TP, Branchek TA, Gerald C, Vaysse PJ, Forray C. 2002. Antidepressant, anxiolytic and anorectic effects of a melanin-concentrating hormone-1 receptor antagonist. Nat Med 8:825–830.

Boutrel B, Kenny PJ, Specio SE, Martin-Fardon R, Markou A, Koob GF, de Lecea L. 2005. Role for hypocretin in mediating stress-induced reinstatement of cocaine-seeking behavior. Proc Natl Acad Sci U S A 102:19168–19173.

Brischoux F, Cvetkovic V, Griffond B, Fellmann D, Risold PY. 2002. Time of genesis determines projection and neurokinin-3 expression patterns of diencephalic neurons containing melanin-concentrating hormone. Eur J Neurosci 16:1672–1680.

Broberger C, De Lecea L, Sutcliffe JG, Hokfelt T. 1998. Hypocretin/orexin- and melanin-concentrating hormone-expressing cells form distinct populations in the rodent lateral hypothalamus: relationship to the neuropeptide Y and agouti gene-related protein systems. J Comp Neurol 402:460–474.

Card JP, Rinaman L, Lynn RB, Lee BH, Meade RP, Miselis RR, Enquist LW. 1993. Pseudorabies virus infection of the rat central nervous system: ultrastructural characterization of viral replication, transport, and pathogenesis. J Neurosci 13:2515–2539.

Cvetkovic V, Brischoux F, Jacquemard C, Fellmann D, Griffond B, Risold PY. 2004. Characterization of subpopulations of neurons producing melanin-concentrating hormone in the rat ventral diencephalon. J Neurochem 91:911–919.

de Lecea L, Kilduff TS, Peyron C, Gao X, Foye PE, Danielson PE, Fukuhara C, Battenberg EL, Gautvik VT, Bartlett FS 2nd, Frankel WN, van den Pol AN, Bloom FE, Gautvik KM, Sutcliffe JG. 1998. The hypocretins: hypothalamus-specific peptides with neuroexcitatory activity. Proc Natl Acad Sci U S A 95:322–327.

Demmin GL, Clase AC, Randall JA, Enquist LW, Banfield BW. 2001. Insertions in the gG gene of pseudorabies virus reduce expression of the upstream Us3 protein and inhibit cell-to-cell spread of virus infection. J Virol 75:10856–10869.

Edwards CM, Abusnana S, Sunter D, Murphy KG, Ghatei MA, Bloom SR. 1999. The effect of the orexins on food intake: comparison with neuropeptide Y, melanin-concentrating hormone and galanin. J Endocrinol 160:R7–12.

Elias CF, Saper CB, Maratos-Flier E, Tritos NA, Lee C, Kelly J, Tatro JB, Hoffman GE, Ollmann MM, Barsh GS, Sakurai T, Yanagisawa M, Elmquist JK. 1998. Chemically defined projections linking the mediobasal hypothalamus and the lateral hypothalamic area. J Comp Neurol 402:442–459.

Enquist LW, Husak PJ, Banfield BW, Smith GA. 1998. Infection and spread of alphaherpesviruses in the nervous system. Adv Virus Res 51:237–347.

Geerling JC, Mettenleiter TC, Loewy AD. 2003. Orexin neurons project to diverse sympathetic outflow systems. Neurosci 122:541–550.

Haring JH, Davis JN. 1983. Acetylcholinesterase neurons in the lateral hypothalamus project to the spinal cord. Brain Res 268:275–283.

Harris GC, Wimmer M, Aston-Jones G. 2005. A role for lateral hypothalamic orexin neurons in reward seeking. Nature 437:556–559.

Harthoorn LF, Sane A, Nethe M, Van Heerikhuize JJ. 2005. Multitranscriptional profiling of melanin-concentrating hormone and orexin-containing neurons. Cell Mol Neurobiol 25:1209–1223.

Haynes AC, Jackson B, Chapman H, Tadayyon M, Johns A, Porter RA, Arch JR. 2000. A selective orexin-1 receptor antagonist reduces food consumption in male and female rats. Regul Pept 96:45–51.

Haynes AC, Chapman H, Taylor C, Moore GB, Cawthorne MA, Tadayyon M, Clapham JC, Arch JR. 2002. Anorectic, thermogenic and anti-obesity activity of a selective orexin-1 receptor antagonist in ob/ob mice. Regul Pept 104:153–159.

Herman JP, Cullinan WE. 1997. Neurocircuitry of stress: central control of the hypothalamo-pituitary-adrenocortical axis. Trends Neurosci 20: 78–84.

Hervieu GJ. 2006. Further insights into the neurobiology of melanin-concentrating hormone in energy and mood balances. Expert Opin Ther Targets 10:211–229.

Hosoya Y. 1980. The distribution of spinal projection neurons in the hypothalamus of the rat, studied with the HRP method. Exp Brain Res 40:79–87.

Hosoya Y. 1985. Hypothalamic projections to the ventral medulla oblongata in the rat, with special reference to the nucleus raphe pallidus: a study using autoradiographic and HRP techniques. Brain Res 344: 338–350.

Jänig W, McLachlan EM. 1992. Characteristics of function-specific pathways in the sympathetic nervous system. Trends Neurosci 15:475–481.

Kayaba Y, Nakamura A, Kasuya Y, Ohuchi T, Yanagisawa M, Komuro I, Fukuda Y, Kuwaki T. 2003. Attenuated defense response and low basal blood pressure in orexin knockout mice. Am J Physiol Regul Integr Comp Physiol 285:R581–593.

Keay KA, Bandler R. 2004. Periaqueductal gray. In: Paxinos G, editor. The rat nervous system, 3rd ed. San Diego, CA: Elsevier. p 243–257.

Kerman IA, Enquist LW, Watson SJ, Yates BJ. 2003. Brainstem substrates of sympatho-motor circuitry identified using trans-synaptic tracing with pseudorabies virus recombinants. J Neurosci 23:4657–4666.

Kerman IA, Akil H, Watson SJ. 2006a. Rostral elements of sympathomotor circuitry: a virally mediated transsynaptic tracing study. J Neurosci 26:3423–3433.

Kerman IA, Shabrang C, Taylor L, Akil H, Watson SJ. 2006b. Relationship of presympathetic-premotor neurons to the serotonergic transmitter system in the rat brainstem. J Comp Neurol 499:882–896.

Kim JS, Enquist LW, Card JP. 1999. Circuit-specific coinfection of neurons in the rat central nervous system with two pseudorabies virus recombinants. J Virol 73:9521–9531.

Kohler C, Haglund L, Swanson LW. 1984. A diffuse alpha MSH-immunoreactive projection to the hippocampus and spinal cord from individual neurons in the lateral hypothalamic area and zona incerta. J Comp Neurol 223:501–514.

Krout KE, Mettenleiter TC, Loewy AD. 2003. Single CNS neurons link both central motor and cardiosympathetic systems: a double-virus tracing study. Neuroscience 118:853–866.

Marsh DJ, Weingarth DT, Novi DE, Chen HY, Trumbauer ME, Chen AS, Guan XM, Jiang MM, Feng Y, Camacho RE, Shen Z, Frazier EG, Yu H, Metzger JM, Kuca SJ, Shearman LP, Gopal-Truter S, MacNeil DJ, Strack AM, MacIntyre DE, Van der Ploeg LH, Qian S. 2002. Melanin-concentrating hormone 1 receptor-deficient mice are lean, hyperactive, and hyperphagic and have altered metabolism. Proc Natl Acad Sci U S A 99:3240–3245.

McLean IW, Nakane PK. 1974. Periodate-lysine-paraformaldehyde fixative. A new fixation for immunoelectron microscopy. J Histochem Cytochem 22:1077–1083.

Messina MM, Overton JM. 2007. Cardiovascular effects of melanin-concentrating hormone. Regul Pept 139:23–30.

Nambu T, Sakurai T, Mizukami K, Hosoya Y, Yanagisawa M, Goto K.

1999. Distribution of orexin neurons in the adult rat brain. Brain Res 827:243–260.

Narita M, Nagumo Y, Hashimoto S, Narita M, Khotib J, Miyatake M, Sakurai T, Yanagisawa M, Nakamachi T, Shioda S, Suzuki T. 2006. Direct involvement of orexinergic systems in the activation of the mesolimbic dopamine pathway and related behaviors induced by morphine. J Neurosci 26:398–405.

Pajolla GP, de Aguiar Correa FM. 2004. Cardiovascular responses to the injection of L-glutamate in the lateral hypothalamus of unanesthetized or anesthetized rats. Auton Neurosci 116:19–29.

Pissios P, Bradley RL, Maratos-Flier E. 2006. Expanding the scales: The multiple roles of MCH in regulating energy balance and other biological functions. Endocr Rev 27:606–620.

Porter JP, Brody MJ. 1986. A comparison of the hemodynamic effects produced by electrical stimulation of subnuclei of the paraventricular nucleus. Brain Res 375:20–29.

Reyes TM, Walker JR, DeCino C, Hogenesch JB, Sawchenko PE. 2003. Categorically distinct acute stressors elicit dissimilar transcriptional profiles in the paraventricular nucleus of the hypothalamus. J Neurosci 23:5607–5616.

Sakurai T. 2007. The neural circuit of orexin (hypocretin): maintaining sleep and wakefulness. Nat Rev Neurosci 8:171–181.

Sakurai T, Amemiya A, Ishii M, Matsuzaki I, Chemelli RM, Tanaka H, Williams SC, Richardson JA, Kozlowski GP, Wilson S, Arch JR, Buckingham RE, Haynes AC, Carr SA, Annan RS, McNulty DE, Liu WS, Terrett JA, Elshourbagy NA, Bergsma DJ, Yanagisawa M. 1998. Orexins and orexin receptors: a family of hypothalamic neuropeptides and G protein-coupled receptors that regulate feeding behavior. Cell 92:573–585.

Samson WK, Bagley SL, Ferguson AV, White MM. 2007. Hypocretin/orexin type 1 receptor in brain: role in cardiovascular control and the neuroendocrine response to immobilization stress. Am J Physiol Regul Integr Comp Physiol 292:R382–387.

Segal-Lieberman G, Bradley RL, Kokkotou E, Carlson M, Trombly DJ, Wang X, Bates S, Myers MG, Jr., Flier JS, Maratos-Flier E. 2003. Melanin-concentrating hormone is a critical mediator of the leptin-deficient phenotype. Proc Natl Acad Sci U S A 100:10085–10090.

Shiosaka S, Kawai Y, Shibasaki T, Tohyama M. 1985. The descending alpha-MSHergic (alpha-melanocyte-stimulating hormone-ergic) projections from the zona incerta and lateral hypothalamic area to the inferior colliculus and spinal cord in the rat. Brain Res 338:371–375.

Smith BN, Banfield BW, Smeraski CA, Wilcox CL, Dudek FE, Enquist LW, Pickard GE. 2000. Pseudorabies virus expressing enhanced green fluorescent protein: a tool for in vitro electrophysiological analysis of transsynaptically labeled neurons in identified central nervous system circuits. Proc Natl Acad Sci U S A 97:9264–9269.

Smith DG, Davis RJ, Rorick-Kehn L, Morin M, Witkin JM, McKinzie DL, Nomikos GG, Gehlert DR. 2006. Melanin-concentrating hormone-1 receptor modulates neuroendocrine, behavioral, and corticolimbic neurochemical stress responses in mice. Neuropsychopharmacology 31: 1135–1145.

Standish A, Enquist LW, Miselis RR, Schwaber JS. 1995. Dendritic morphology of cardiac related medullary neurons defined by circuit-specific infection by a recombinant pseudorabies virus expressing beta-galactosidase. J Neurovirol 1:359–368.

Swanson LW. 2004. Brain maps: structure of the rat brain. San Diego, CA: Elsevier Academic Press.

Swanson LW, Kuypers HG. 1980. The paraventricular nucleus of the hypothalamus: cytoarchitectonic subdivisions and organization of projections to the pituitary, dorsal vagal complex, and spinal cord as demonstrated by retrograde fluorescence double-labeling methods. J Comp Neurol 194:555–570.

Swanson LW, Sanchez-Watts G, Watts AG. 2005. Comparison of melanin-concentrating hormone and hypocretin/orexin mRNA expression patterns in a new parceling scheme of the lateral hypothalamic zone. Neurosci Lett 387:80–84.

Vahlne A, Nystrom B, Sandberg M, Hamberger A, Lycke E. 1978. Attachment of herpes simplex virus to neurons and glial cells. J Gen Virol 40:359–371.

Vahlne A, Svennerholm B, Sandberg M, Hamberger A, Lycke E. 1980. Differences in attachment between herpes simplex type 1 and type 2 viruses to neurons and glial cells. Infect Immun 28:675–680.

van den Pol AN. 1999. Hypothalamic hypocretin (orexin): robust innervation of the spinal cord. J Neurosci 19:3171–3182.

Verret L, Goutagny R, Fort P, Cagnon L, Salvert D, Leger L, Boissard R, Salin P, Peyron C, Luppi PH. 2003. A role of melanin-concentrating hormone producing neurons in the central regulation of paradoxical sleep. BMC Neurosci 4:19.

Willie JT, Chemelli RM, Sinton CM, Yanagisawa M. 2001. To eat or to sleep? Orexin in the regulation of feeding and wakefulness. Annu Rev Neurosci 24:429–458.

Winsky-Sommerer R, Yamanaka A, Diano S, Borok E, Roberts AJ, Sakurai T, Kilduff TS, Horvath TL, de Lecea L. 2004. Interaction between the corticotropin-releasing factor system and hypocretins (orexins): a novel circuit mediating stress response. J Neurosci 24:11439–11448.

Yamanaka A, Beuckmann CT, Willie JT, Hara J, Tsujino N, Mieda M, Tominaga M, Yagami K, Sugiyama F, Goto K, Yanagisawa M, Sakurai T. 2003. Hypothalamic orexin neurons regulate arousal according to energy balance in mice. Neuron 38:701–713.

Zhang W, Shimoyama M, Fukuda Y, Kuwaki T. 2006. Multiple components of the defense response depend on orexin: evidence from orexin knockout mice and orexin neuron-ablated mice. Auton Neurosci 126–127: 139–145.

Zhou D, Shen Z, Strack AM, Marsh DJ, Shearman LP. 2005. Enhanced running wheel activity of both Mch1r- and Pmch-deficient mice. Regul Pept 124:53–63.